

Figure S1. Spatial distribution of land cover type in Amazon with 0.25° spatial resolution in 2018.

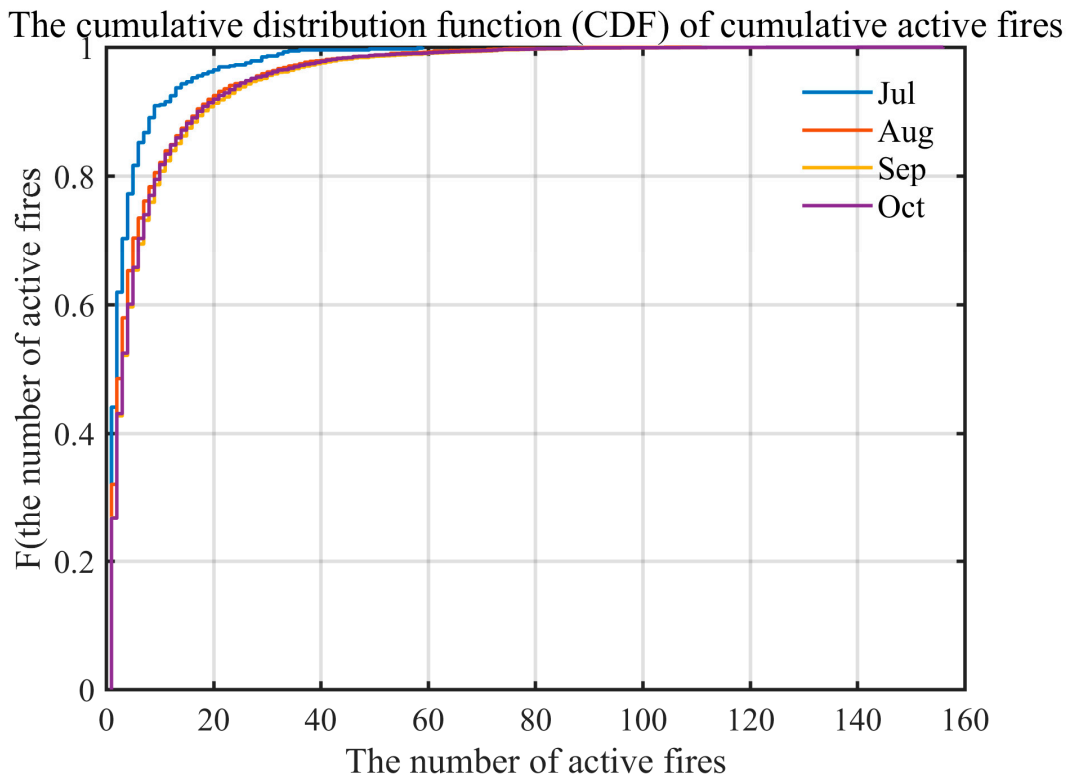


Figure S2. The cumulative distribution function (CDF) of cumulative active fires from July to October. We classified the fire events into 10 levels based on 10% intervals according to the cumulative distribution function (CDF) of cumulative active fires data from July to September. The CDF of active fires in the whole fire season (purple line) showed that 50% of pixels had fewer than three active fires and 20% of pixels had fewer than 10 active fires. There was around 1–2 pixels in each higher number of active fires (active fires > 20). If we used 5% intervals to classify fire events, there would be fewer pixels and a higher number of active fires, which was not sufficient to give an average to stand for the general canopy change at some levels

due to the effect of different species. Thus, we chose 10% as an interval to classify the fire events into 10 levels.

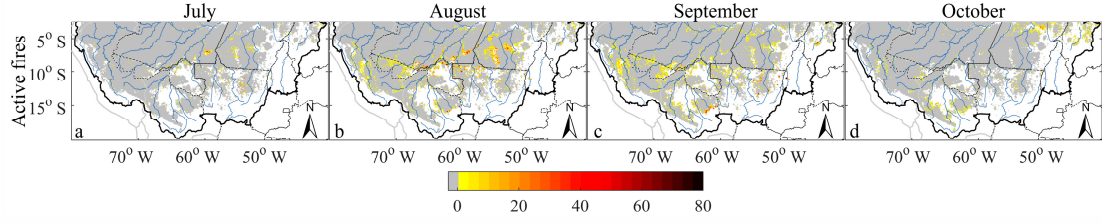


Figure S3. Spatial distribution of active fires on 0.1° grid cells from July to October 2019.

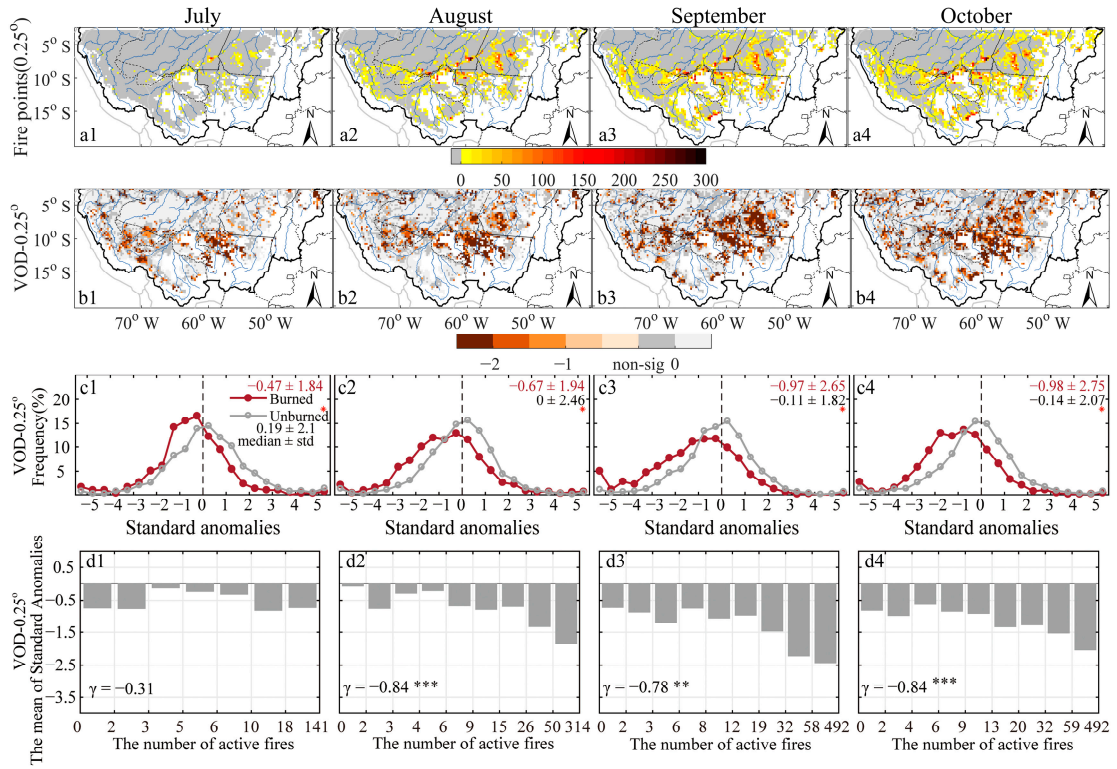


Figure S4. Spatial distribution of cumulative active fires on 0.1° (a1–a4) grid cells from July to October 2019. Spatial distribution of standardized anomalies in (b1–b4) VOD-0.25° from July to October 2019. Histograms of standardized anomalies from July to October in (c1–c4) VOD-0.25. Red asterisks indicated that the anomalies between burned and unburned pixels were significantly different. The mean standard anomalies of (d1–d4) VOD-0.25° at different fire situation levels from July to October 2019. Significant Pearson correlation coefficient ($p < 0.1$, $p < 0.05$ and $p < 0.01$) was indicated with *, **, and ***, respectively.

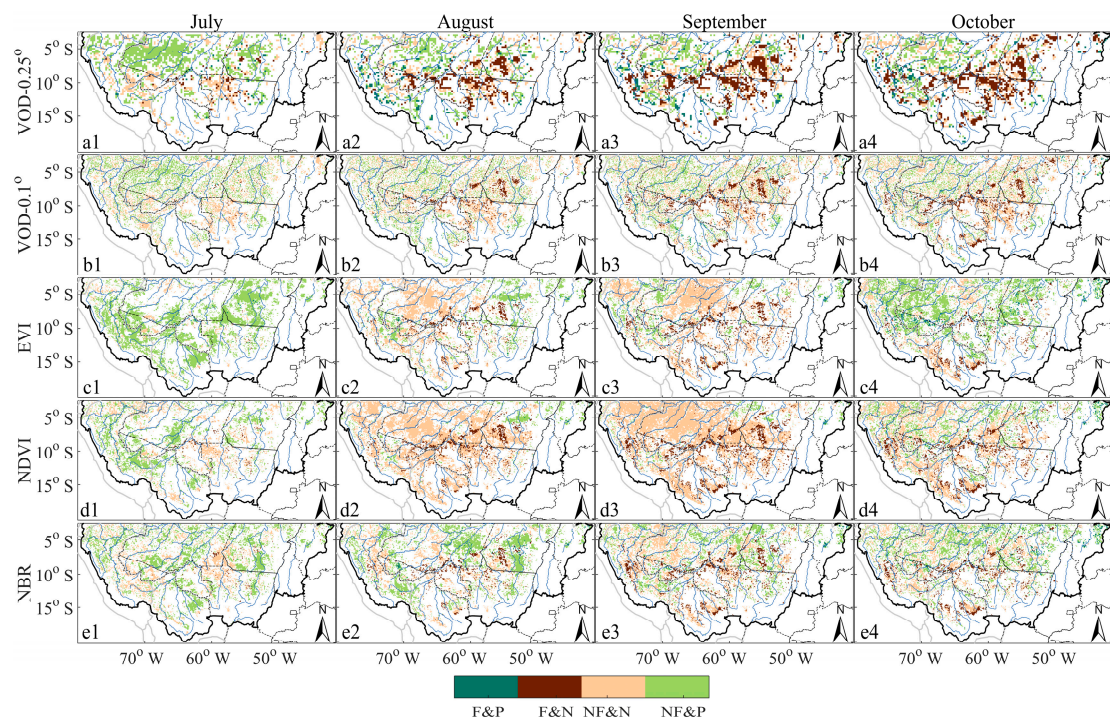


Figure S5. A comparison of the locations of burned pixels and significant (a1–a4) VOD-0.25°, (b1–b4) VOD-0.1°, (c1–c4) EVI, (d1–d4) NDVI, (e1–e4) NBR anomalies pixels from July to October 2019. F&P referred to burned pixels with positive remote sense indices anomalies. F&N referred to burned pixels with negative remote sense indices anomalies. NF&N referred to unburned pixels with negative remote sense indices anomalies. NF&P referred to unburned pixels with positive remote sense indices anomalies.

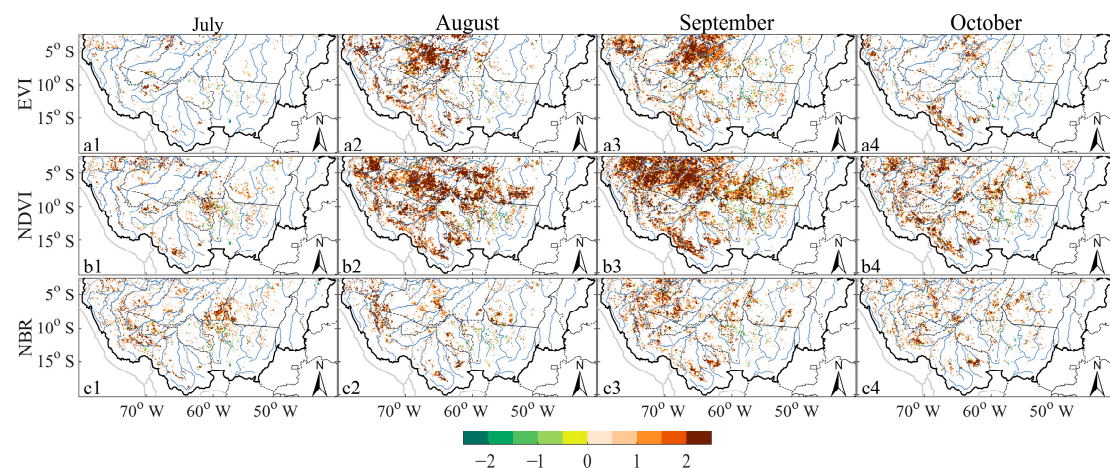


Figure S6. The absolute value difference of significant negative anomalies between optical indices and VOD-0.1° in unburned pixels from July to October 2019.

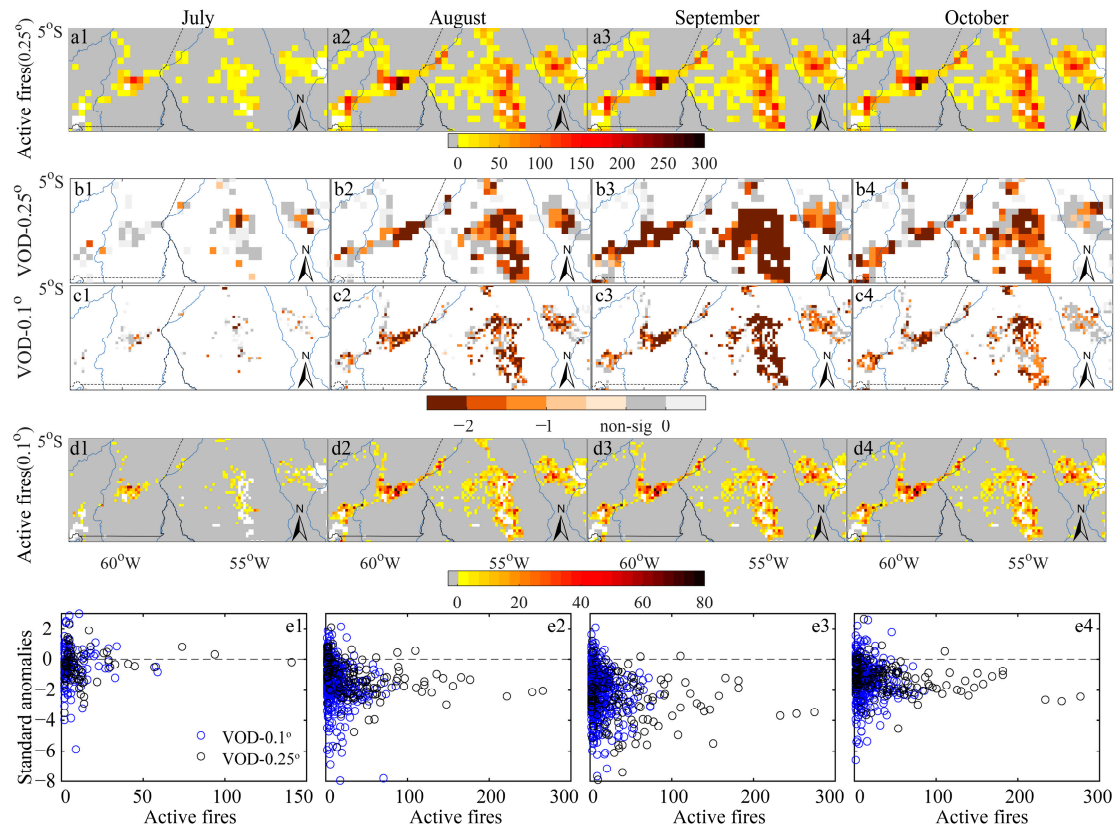


Figure S7. A comparison of standard anomalies between fire data and VOD at different resolutions in the higher fire occurrence areas (5° – 9° S, 52° – 62° W) from July to October 2019. (a1–a4) and (d1–d4) was the spatial distribution of cumulative active fires with high-level confidence on 0.25° and 0.1° grid cells. (b1–b4) and (c1–c4) was the spatial distribution of standardized anomalies in VOD at low (0.25°) and high resolution (0.1°). The scatter plots of standard anomalies varied with active fires (e1–e4).

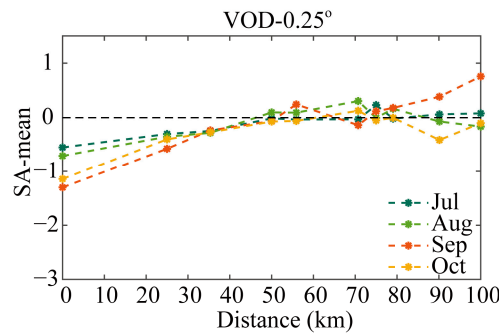


Figure S8. The mean of standard anomalies (SA-mean) of VOD- 0.25° in unburned pixels at different distances from burned pixels.

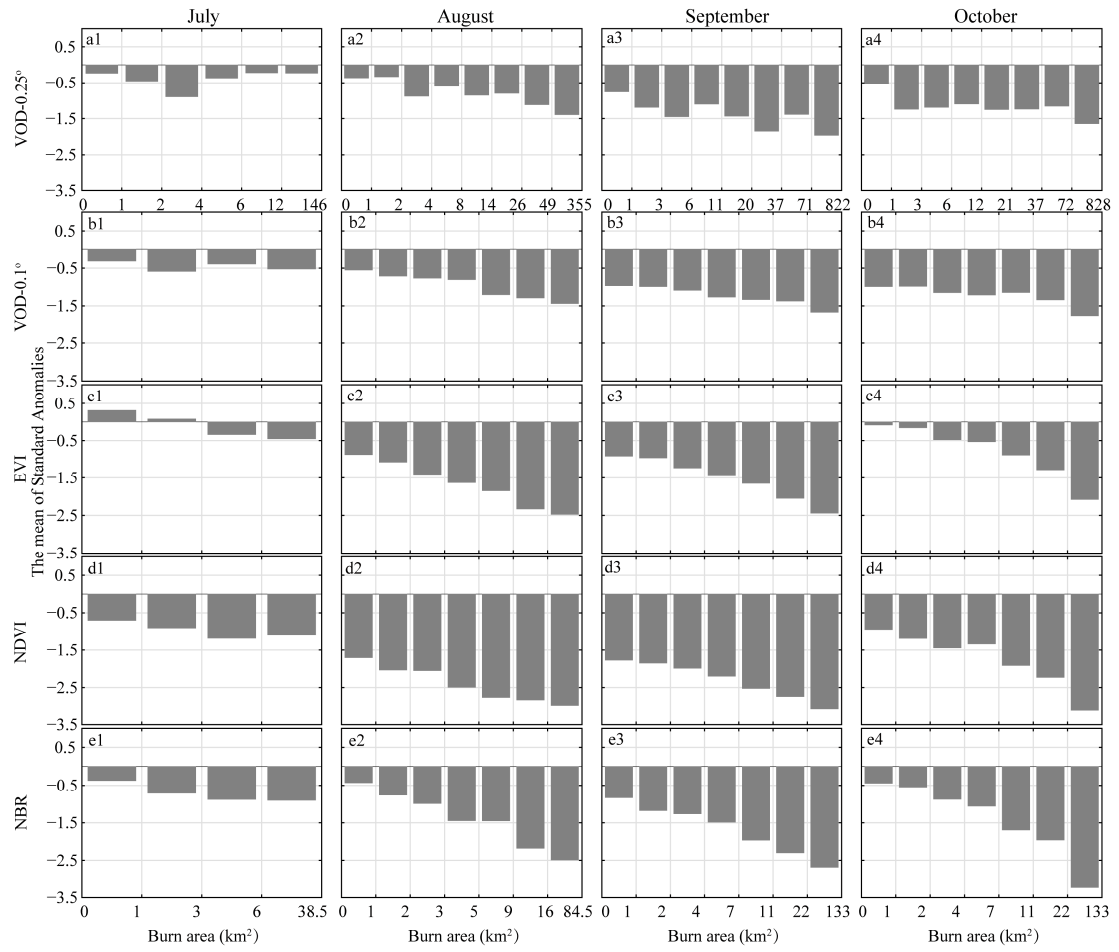


Figure S9. The mean standard anomalies of (a1–a4) VOD-0.25°, (b1–b4) VOD-0.1°, (c1–c4) EVI, (d1–d4) NDVI, and (e1–e4) NBR at different burn area levels from July to October 2019.

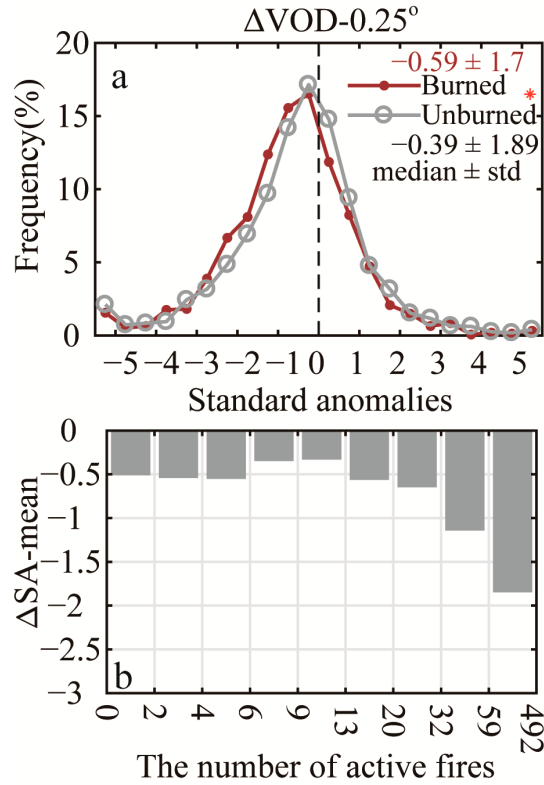


Figure S10. The comparison of ΔVM ($\Delta VM = VM_{Oct} - VM_{Jul}$) standardized anomalies' distribution between burned and unburned areas. Histograms of standardized anomalies in $\Delta VOD-0.25^\circ$ (a). A red asterisk indicated that the anomalies between burned and unburned pixels were significantly different. The mean of standard anomalies of $\Delta VOD-0.25^\circ$ (b) at different fire event levels.

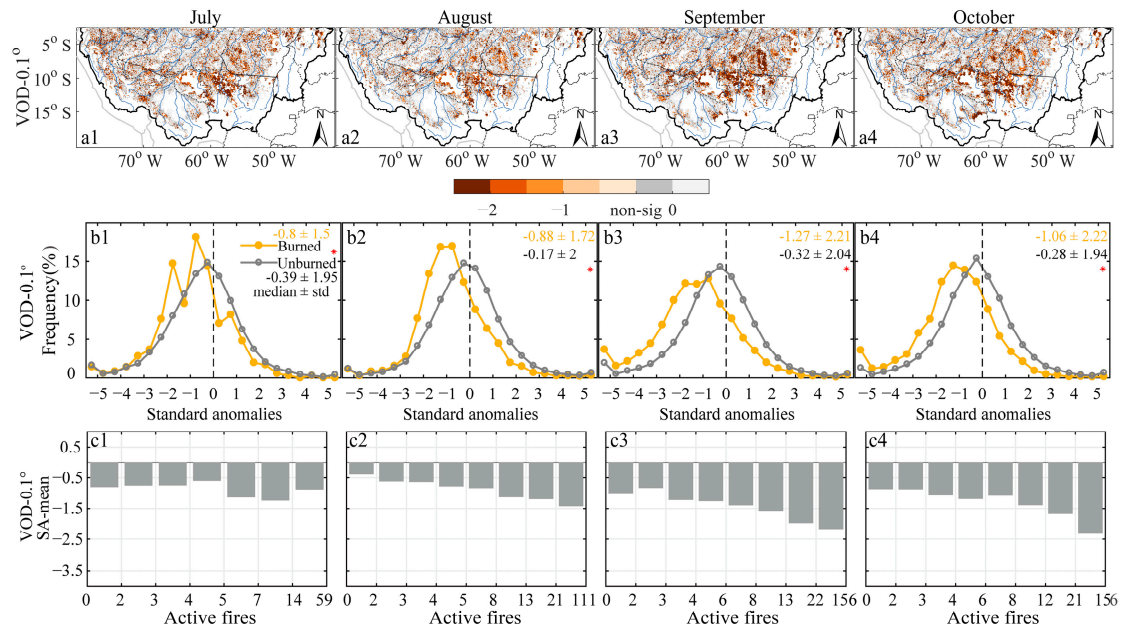


Figure S11. Spatial distribution of standardized anomalies in $VOD-0.1^\circ$ based on

daytime passive microwave observation (named VOD-0.1°-A here, **a1–a4**) from July to October 2019. Histograms of standardized anomalies from July to October in VOD-0.1°-A (**b1–b4**). Red asterisks indicated that the anomalies between burned and unburned pixels were significantly different. The mean standard anomalies of VOD-0.1°-A (**c1–c4**) at different fire situation levels from July to October 2019.

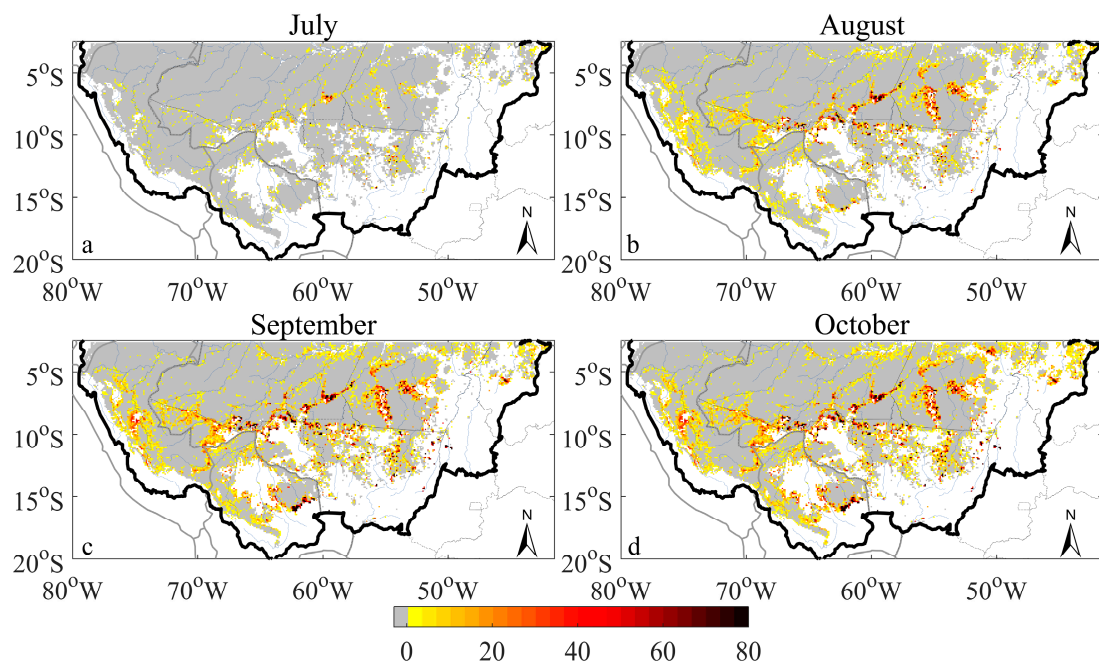


Figure S12. Spatial distribution of cumulative active fires with all confidence levels on 0.1° grid cells from July to October 2019.

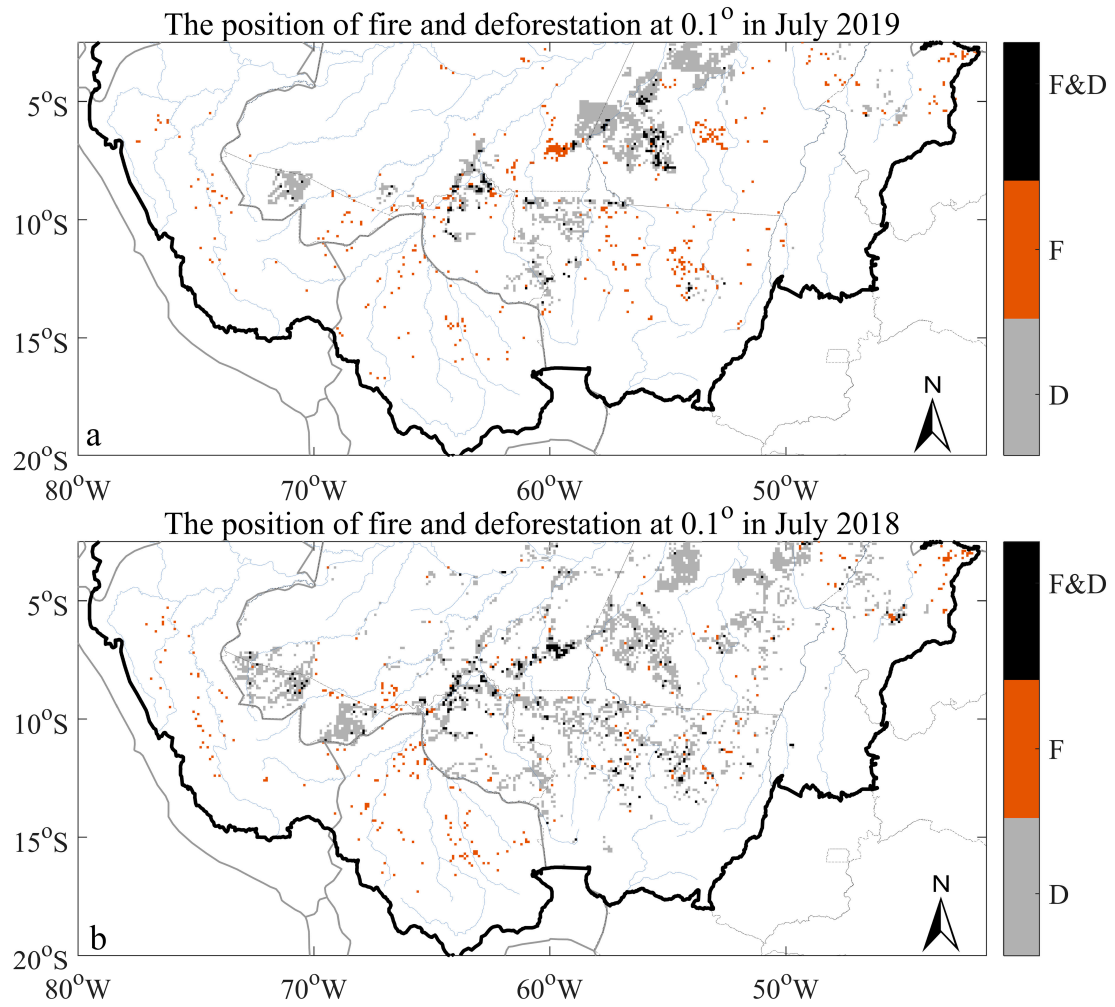


Figure S13. A comparison of the locations of burned pixels and deforested pixel in (a) July 2019 and (b) July 2018. F&D referred to burned pixels with deforested. F referred to burned pixels with no deforested. D referred to deforested pixel with no fire.